Muon spin rotation study of magnetism in electron-doped chromium sulfide

M. L. Brooks, S. J. Blundell, C. A. Steer, and T. Lancaster
Clarendon Laboratory, University of Oxford, Parks Road, Oxford, OX1 3PU, United Kingdom

F. L. Pratt
ISIS Facility, Rutherford Appleton Laboratory, Chilton, Oxfordshire OX11 0QX, United Kingdom

P. Vaqueiro and A. V. Powell
Department of Chemistry, Heriot-Watt University, Edinburgh EH14 4AS, United Kingdom
(Received 5 March 2005; published 28 July 2005)

We report the results of a muon spin rotation study on electron-doped chromium sulfides, Cr_2S_{3-x}, with $0 \leqslant x \leqslant 0.08$. Two muon-spin precession frequencies are observed in each sample, corresponding to two distinct stopping sites. We show that even a small amount of electron doping, induced by sulfur deficiency, causes a drastic change in the magnetic properties.

DOI: 10.1103/PhysRevB.72.012419 PACS number(s): 76.75.+i, 75.47.Gk, 75.30.−m, 75.50.−y

The discovery of colossal magnetoresistance (CMR) in the perovskite manganates has led to renewed interest in mixed-valence systems.[1] For the manganates, CMR has been described in terms of a double-exchange mechanism involving ferromagnetic alignment of neighboring Mn^{3+} ($3d^4$) and Mn^{4+} ($3d^3$) ions that enhances charge transport. CMR is found in other systems, including the pyrochlore oxides, such as $Tl_2Mn_2O_7$,[2] the layered iodide GdI_2,[3] chromium chalcogenide spinels ACr_2X_4 (A=Cd, Fe; X=S, Se, Te),[4] and sulfur-deficient rhombohedral Cr_2S_{3-x}.[5] For this last system, stoichiometric Cr_2S_3 contains only Cr^{3+} ions, so that the mixed-valence arises when $x>0$ due to the sulfur deficiency which introduces an excess of electrons and creates formally a small amount of Cr^{2+}. Therefore, this material shares with the manganates the presence of both Jahn-Teller (Cr^{2+},$3d^4$) and non-Jahn-Teller (Cr^{3+},$3d^3$) species. Stoichiometric Cr_2S_3 has a structure in which the building blocks are chromium-centered sulfur octahedra. Edge sharing of octahedra generates CrS_2 slabs separated by a layer containing a network of octahedral sites, one third of which are occupied by additional chromium ions. Ordering of the vacancies within this layer leads to a two-dimensional superstructure. Trimers of face-sharing octahedra serve to link the CrS_2 slabs.[6]

Magnetization measurements show Cr_2S_3 to be a weak ferrimagnet (T_N=118 K) but neutron-diffraction reveals three distinct magnetic sublattices arranged such that complete cancellation of moments, and antiferromagnetic behavior, is expected.[7] It was then proposed that ferrimagnetism arises because of spins canting out of the *ab* plane,[7] but a further study suggested it may be due to differences in the occupancies of the three crystallographically distinct Cr sites.[8] Transport measurements show it to be an insulator. In contrast, sulfur-deficient samples (Cr_2S_{3-x}, $x>0$) are much less resistive and show significant magnetoresistance near T_N. Measurements performed on the nonstoichiometric compound $Cr_2S_{2.92}$ (Ref. 5) were analyzed in terms of conduction by both bare electrons and magnetic polarons; x-ray and neutron diffraction measurements suggest that the sulfur deficiency results in incorporation of excess chromium at a fraction of the normally vacant sites in the defective layer.[9]

In this paper, we present the results of zero-field muon spin rotation (μSR) experiments performed on samples of rhombohedral chromium sulfide, Cr_2S_{3-x}, with $0<x<0.08$. In contrast with earlier μSR experiments[5] performed at a pulsed muon source, these new measurements have been performed using a continuous muon source which allows sufficient time resolution to follow the temperature dependence of the internal field directly.

Polycrystalline samples of Cr_2S_{3-x} with $0<x<0.08$ were prepared by heating an appropriate mixture of the elements in a sealed evacuated silica tube ($<10^{-4}$ torr) at 500 °C for 24 h and then at 800 °C for 4 days. After regrinding, the powders were pressed into pellets and refired at 1000 °C for 4 days before cooling to room temperature at 4 K min^{-1} (see Ref. 5). Powder x-ray diffraction data confirmed that the materials are single phase with lattice parameters similar to those reported by Jellinek[6] for rhombohedral Cr_2S_3. The μSR experiments were carried out on the DOLLY spectrometer at the Paul Scherrer Institute (PSI), Villigen, Switzerland. In our μSR (Ref. 10) experiment, each sample was mounted on a silver backing plate and spin polarized positive muons (μ^+, momentum 28 MeV/c) were implanted. The time evolution of the muon-spin polarization is obtained by counting emitted decay positrons forward (f) and backward (b) of the initial muon spin direction; this is possible due to the asymmetric nature of the muon decay,[10] which takes place in a mean time of 2.2 μs. We record the number of positrons detected by forward (N_f) and backward (N_b) counters as a function of time and calculate the asymmetry function, $A(t)$, defined by

$$A(t) = \frac{N_f(t) - \alpha_{exp} N_b(t)}{N_f(t) + \alpha_{exp} N_b(t)}, \quad (1)$$

where α_{exp} is an experimental calibration constant and differs from unity due to nonuniform detector efficiency. The quantity $A(t)$ is proportional to the average spin polarization, $P_z(t)$, of muons stopping within the sample. The muon spin precesses around a local magnetic field, B (with an angular frequency $\gamma_\mu|B|$, where $\gamma_\mu = 2\pi \times 135.5$ MHz T^{-1}), and so following implantation into a powdered material that pre-

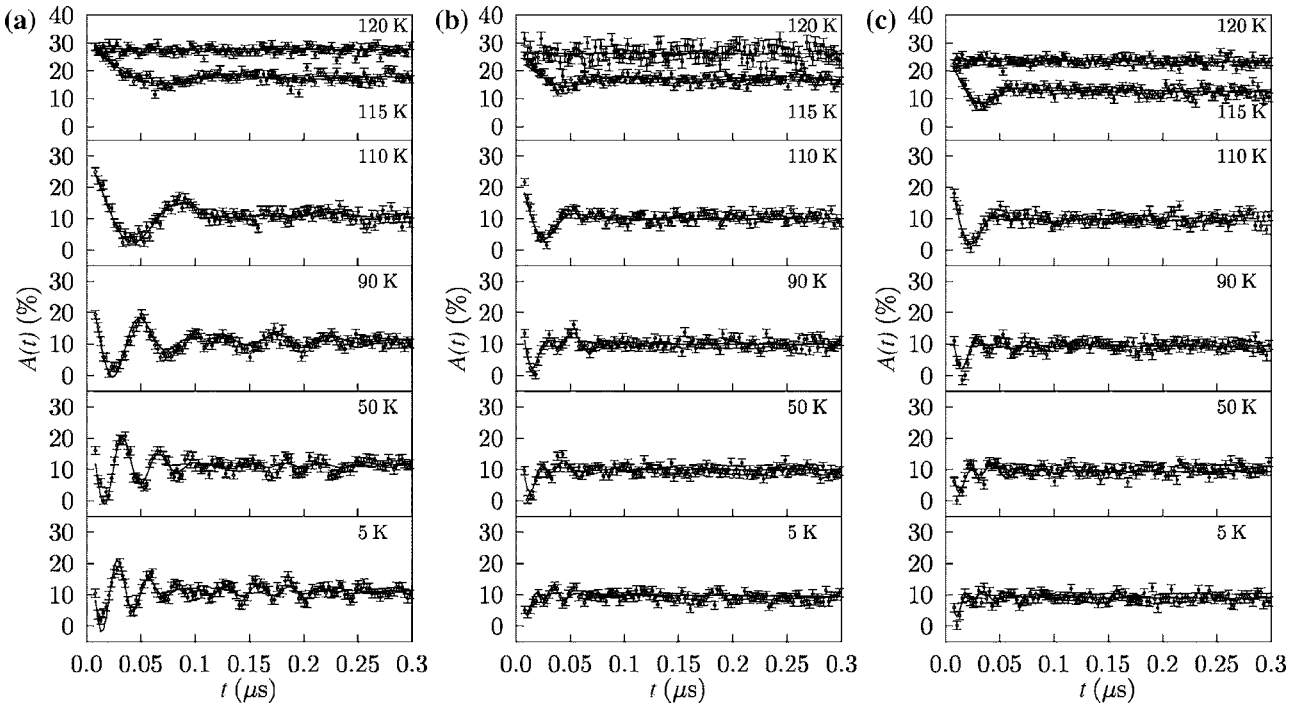

FIG. 1. Muon decay asymmetry plots for (a) Cr_2S_3, (b) $Cr_2S_{2.96}$, and (c) $Cr_2S_{2.92}$. The solid lines are fits to Eq. (2).

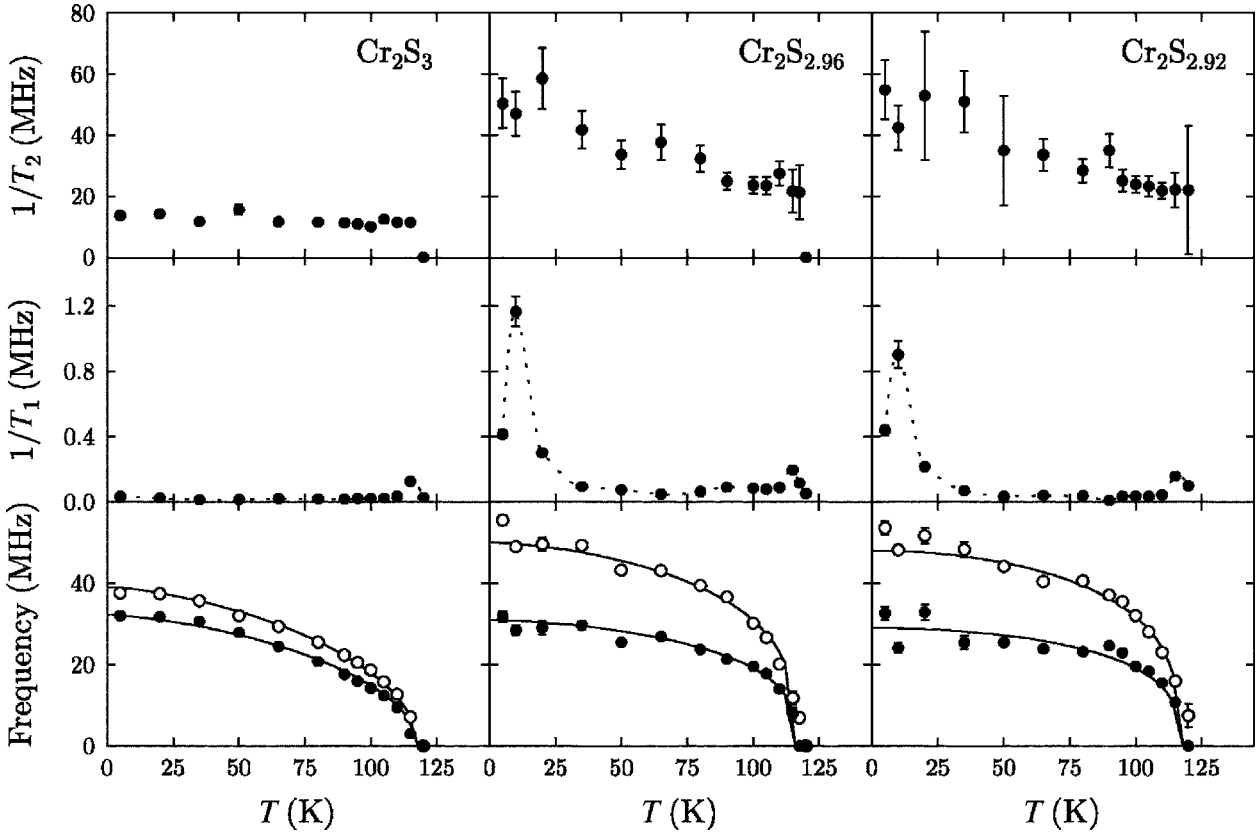

FIG. 2. Plots of the parameters used to fit Eq. (2) to the muon asymmetry spectra. The solid lines in the frequency plots are fits to the phenomenological magnetization [Eq. (3)], and the dotted lines in the $1/T_1$ plots are guides for the eye.

TABLE I. Parameters of best fits of the oscillation frequency data to the phenomenological magnetization function equation (3).

Parameter	Cr_2S_3	$Cr_2S_{2.96}$	$Cr_2S_{2.92}$
A_1/A_{tot} (%)	30.9(4)	37.6(5)	38(1)
A_2/A_{tot} (%)	35.7(4)	35.7(5)	39(1)
$\nu_1(0)$ (MHz)	39.0(6)	50(1)	48(2)
$\nu_2(0)$ (MHz)	32.2(5)	31(1)	29(1)
α	1.5(2)	1.6(4)	2.0(7)
β	0.51(4)	0.32(4)	0.31(6)
T_N (K)	118(1)	116(1)	117(1)

sents a quasi-static field at the stopping site, the muon will precess around the component of the local field that is perpendicular to its spin direction.

Examples of raw asymmetry spectra measured on samples with $x=0, 0.04$, and 0.08 are plotted in Fig. 1. At low temperatures, the data for Cr_2S_3 [Fig. 1(a)] clearly show an oscillating signal with a beating amplitude due to the presence of two frequencies. This is superposed on a much slower exponential relaxation. The muon precession frequencies both decrease with increasing temperature. Near to T_N the slow exponential relaxation begins to account for a greater fraction of the asymmetry and at 120 K the oscillating signal is no longer observed. These are the usual changes associated with a transition from a magnetically ordered state to a paramagnetic one.

The data for the sulfur-deficient compounds [Figs. 1(b) and 1(c)] show the same general trend, but the oscillations have higher frequencies and are more strongly damped. In order to parametrize the data for all samples, they were fitted to the functional form

$$A(t) = A_{bg} + A_{exp}\exp\left(-\frac{t}{T_1}\right) + \exp\left(-\frac{t}{T_2}\right) \times [A_1\cos(2\pi\nu_1 t) + A_2\cos(2\pi\nu_2 t)], \quad (2)$$

where A_{bg} is a time-independent background due to muons

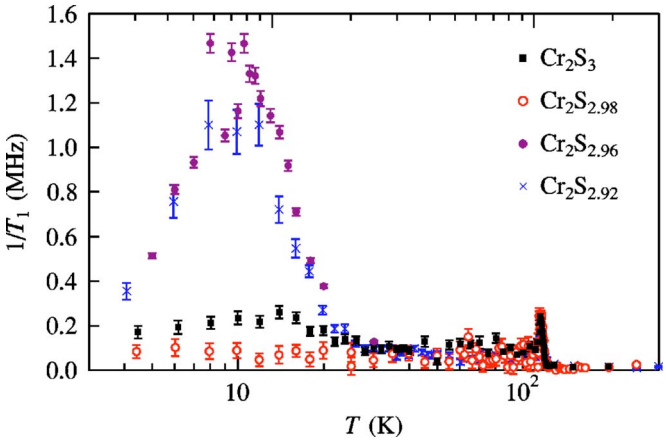

FIG. 3. (Color online) Relaxation rate extracted from fits of a simple exponential to ISIS data measured for Cr_2S_3, $Cr_2S_{2.98}$, and $Cr_2S_{2.92}$ (Ref. 5) and PSI data for $Cr_2S_{2.96}$.

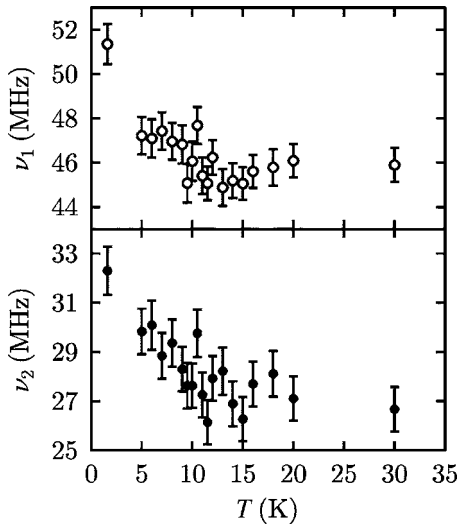

FIG. 4. Oscillation frequencies extracted from fits of Eq. (2) to data measured for $Cr_2S_{2.96}$.

stopping in the silver that surrounds the sample, $\nu_{1,2}$ are the two muon precession frequencies ($\nu_1 > \nu_2$) with $A_{1,2}$ their respective amplitudes, and A_{exp} is the amplitude of the slow exponential. $1/T_1$ and $1/T_2$ are the longitudinal[11] and transverse relaxation rates, respectively. A common T_2 for both oscillating components yielded acceptable fits to the data.

Plots of the fitted parameters versus temperature are shown in Fig. 2. The data for Cr_2S_3 clearly show that the magnetic transition is taking place between 115 K and 120 K, as evidenced by the disappearance of the oscillating signal and the appearance of a peak in $1/T_1$. Below the transition, the appearance of both relaxation rates appears to have little dependence on temperature. The oscillation frequencies are proportional to the sublattice magnetization, and its development in temperature is reflected in the plot. Fits to the phenomenological equation

$$\nu_i(T) = \nu_i(0)\left[1 - \left(\frac{T}{T_N}\right)^{\alpha}\right]^{\beta} \quad (3)$$

are shown. These fits (also shown for the other two samples) help to quantify the changes in the shape of the frequency plots, and the fitted parameters are listed in Table I. The fit to the $\nu_i(T)$ data for Cr_2S_3 is better than for the doped samples, with much less scatter about the fit line. This is most likely due to the increased disorder in the latter, which results in a more strongly damped oscillation so that fewer complete cycles of the signal are measured and the extracted frequency is less certain. The derived transition temperatures are in good agreement with the previous work, and the value of α is close to 3/2, which is consistent with the expected behavior of the low temperature magnetization in a ferrimagnet using spin-wave theory.[12]

Plots of fitted parameters for the two sulfur-deficient samples appear very similar. One of the measured frequencies is at approximately the same value as those in Cr_2S_3, but the second one has a higher value.

For rapid fluctuations, the longitudinal relaxation rate is given by

$$\frac{1}{T_1} \propto \gamma_\mu^2 \sum_q |\delta B(q)|^2 \tau(q), \tag{4}$$

where $|\delta B(q)|$ is the amplitude of the fluctuating field at the muon site and $\tau(q)$ is the Cr-ion correlation time; the sum over the wave vector q of excitations is necessary because the muon is a local probe. Near a magnetic phase transition, $\tau(q)$ increases (critical slowing down) and a peak can be observed in $1/T_1$. The transverse relaxation rate $1/T_2$, which measures the spread of the local field in the ordered state, increases as the amount of sulfur is decreased, reflecting the disorder that is introduced into the system with doping. This rate decreases as the temperature is raised.

The plots of $1/T_1$ for the $x>0$ samples still show the peak at the transition, but it is dwarfed by a new peak that appears around 10–15 K. This peak was previously observed in data collected at ISIS (Ref. 5) (see Fig. 3), but an explanation for it had not been found. We performed further measurements near the low temperature peak on the $Cr_2S_{2.96}$ sample at PSI, concentrating on the behavior of the frequencies in this region by fitting only the very early time data ($0<t<0.05$ μs) to Eq. (2). The slow relaxing fraction was ignored by setting $1/T_1$ to zero and absorbing its amplitude into a free parameter A_{bg}. The results are shown in Fig. 4, and hint at a small kink in the temperature dependence of both frequencies near the low temperature peak in $1/T_1$. This demonstrates that the peak in $1/T_1$ is due to a very subtle change in the local magnetic ordering, and probably reflects the freezing out of a small, fluctuating component of the local field which is induced by the magnetic disorder associated with the sulfur deficiency.

Observing the change in the $\nu_i(T)$ plots as the doping level is changed, it is tempting to assign the lowest frequency in the doped samples to the average of the frequencies seen in the undoped material, and then to suggest that the upper frequency corresponds to muons stopping at a site near to an extra chromium ion that the doping introduces. This is not supported by the measured amplitudes of the two oscillating signals; if that were the case one would naïvely expect that the number of muons, and hence the asymmetry fraction, associated with the ν_1 signal would be twice as large in $Cr_2S_{2.92}$ as in $Cr_2S_{2.96}$. Table I shows that the relative amplitudes of the oscillating fractions are very similar in both of these compounds.

In conclusion, μSR experiments were performed on a series of electron-doped chromium sulfide samples. The results demonstrate the development of the sublattice magnetization in each sample and also reflect the disorder introduced into the nonstoichiometric samples. The two sulfur-deficient samples, which show a CMR effect, give rise to muon precession signals that are different from those observed in a stoichiometric sample. This observation emphasizes that a very small move away from stoichiometry has a large effect on the properties of this material. The precession frequency data are nevertheless consistent with a ferrimagnetic ground state. We observe a large peak in the longitudinal relaxation rate centered near 10 K which is most prominent in the most highly sulfur-deficient samples and may reflect the freezing out of a small, fluctuating component of the local field.

Parts of this work were performed at the Swiss Muon Source, Paul Scherrer Institute, Villigen, Switzerland, and at the ISIS Pulsed Muon Facility, UK. We are grateful to P. J. C. King (ISIS) and R. Scheuermann (PSI) for experimental assistance, to A. I. Coldea for useful discussions, and to the EPSRC (UK) for financial support.

[1] M. B. Salamon and M. Jaime, Rev. Mod. Phys. **73**, 583 (2001).
[2] M. Subramanian, B. Toby, A. Ramirez, W. Marshall, A. Sleight, and G. Kwei, Science **273**, 81 (1996).
[3] C. Felser, K. Ahn, R. Kremer, R. Seshadri, and A. Simon, J. Solid State Chem. **147**, 19 (1999).
[4] A. Ramirez, R. Cava, and J. Krajewski, Nature (London) **386**, 156 (1997).
[5] P. Vaqueiro, A. V. Powell, A. I. Coldea, C. A. Steer, I. M. Marshall, S. J. Blundell, J. Singleton, and T. Ohtani, Phys. Rev. B **64**, 132402 (2001).
[6] F. Jellinek, Acta Crystallogr. **10**, 620 (1957).
[7] E. F. Bertaut, J. Cohen, B. Lambert-Andron, and P. Mollard, J. Phys. (Paris) **29**, 813 (1968).
[8] T. J. A. Popma, C. Haas, and B. van Laar, J. Phys. Chem. Solids **32**, 581 (1968).
[9] A. V. Powell (unpublished).
[10] S. J. Blundell, Contemp. Phys. **40**, 175 (1999).
[11] The longitudinal relaxation time was determined by fitting only the first term from 0.3 to 5 μs, then holding it fixed while the entire function was fitted from 0 to 0.3 μs. The sum of the fractional amplitudes was held fixed at a value determined from experimental runs well above the transition temperature (see Table I). It proved possible to keep the values of the other amplitudes fixed, for temperatures in the range $5\ \mathrm{K} \leqslant T \leqslant 110\ \mathrm{K}$, at values determined from earlier fit attempts (see Table I).
[12] W. Marshall and S. W. Lovesey, *Theory of Thermal Neutron Scattering* (Oxford University Press, Oxford, 1971), Sec. 9.7.